

If we consider a realistic, spherical model of Titan's surface and allow that the craters or tidal basins have a spectrum of sizes and that their depths vary with their diameters, then the dissipation rate is determined by the frequency distribution of crater sizes. Observations²¹ of the other satellites of Saturn show that this is well represented by the power law

$$dN = AD^b dD \quad (6)$$

where dN is the number of craters in the diameter range D to $D + dD$ and $b = -3$. The constant A in equation (6) is determined by the normalization requirement that the total area of the craters be comparable with that of the satellite. If the craters range in diameter from D_{\max} to D_{\min} , then $A = 4\pi R_T^2 / \ln(D_{\max}/D_{\min})$ and, if $D_{\max} \approx R_T$ and $D_{\min} \approx 20$ km, then $\ln(D_{\max}/D_{\min}) \approx 5$. If we compare the dissipation rate in a global ocean of depth d_o with that of a cratered satellite on which all the craters have the same depth d_o , then the dissipation rate is reduced by a factor $\sim 6 (1.32R_T/D_{\max})^6 \ln(D_{\max}/D_{\min})$. If the depth d of each crater decreases linearly with its diameter according to $d = (D/D_{\max})d_o$, then the dissipation rate is reduced by a factor $\sim 3 (1.32R_T/D_{\max})^6 \ln(D_{\max}/D_{\min})$. In both cases, the dissipation rate is an average rate but is chiefly determined by the dissipation that occurs in the largest tidal basin. Thus, on Titan, the actual dissipation rate will vary with the location of that largest crater.

This model demonstrates that if the fluid on Titan is confined to shallow seas with sizes smaller than the satellite radius, then as long as the seas are land-locked and disconnected, large liquid hydrocarbon reservoirs, and regions with no liquid hydrocarbons can coexist on the surface of Titan along with a large orbital eccentricity. The recent Hubble Space Telescope observations¹⁰ of Titan show variations in the surface reflectivity of 10–20%. The interpretation of such variations may provide a test of the configuration of land and sea proposed here. The configuration could also be tested by the Arecibo Observatory after its current resurfacing, and by radar and near-infrared observations by the Cassini Saturn Orbiter.

We have assumed that the largest source of tidal dissipation in Titan's ocean is boundary-layer turbulence. Our arguments also apply, however, to any other source of oceanic dissipation that increases with the velocity of the tidal current, for example, dissipation associated with internal waves¹³. Finally, we note that even if oceanic tidal friction is negligible on Titan this may not entirely solve the problem of Titan's high orbital eccentricity because solid body friction may reduce Q_T to a value less than 200 (ref. 22). One possible, but unlikely, solution is that Titan's eccentricity is not primordial but is the result of a recent large, but less than cataclysmic, collision (one less than 10^9 years ago). But even in the most favourable circumstances, this would require Titan to have been struck by, for example, a body with a mass $\sim 0.005M_T$ (or diameter $\sim 10^3$ km) moving with a velocity ~ 15 km s⁻¹ relative to Saturn. No impact basin of appropriate size seems evident in the current infrared data for Titan. □

16. Smith, B. A. *et al.* *Science* **212**, 163–191 (1981).
17. Engel, S., Hartmann, W. K. & Lunine, J. I. (abstr.) *Bull. Am. astr. Soc.* **26**, 1183 (1994).
18. Merian, J. R. *Über die Bewegung tropfbarer Flüssigkeiten in Gefässen* (Basle, 1828).
19. Turcotte, D. L. & Schubert, G. *Geodynamics* (Wiley, New York, 1982).
20. Sagan, C. & Dermott, S. (abstr.) *Bull. Am. astr. Soc.* **26**, 1183 (1994).
21. Chapman, C. R. & McKinnon, W. B. in *Satellites* (eds Burns, J. A. & Matthews, M. S.) 492–580 (Univ. Arizona Press, Tucson, 1986).
22. Peale, S. J., Cassen, P. & Reynolds, R. T. *Icarus* **43**, 65–72 (1980).

ACKNOWLEDGEMENTS. We thank J. Lunine for comments. This work was supported by NASA.

Comb-type grafted hydrogels with rapid de-swelling response to temperature changes

Ryo Yoshida, Katsumi Uchida*, Yuzo Kaneko*, Kiyotaka Sakai*, Akihiko Kikuchi, Yasuhisa Sakurai & Teruo Okano†

Institute of Biomedical Engineering,
Tokyo Women's Medical College, 8-1 Kawada-cho, Shinjuku-ku,
Tokyo 162, Japan

* Department of Chemical Engineering, Waseda University,
3-4-1 Ohkubo, Shinjuku-ku, Tokyo 169, Japan

MANY polymeric hydrogels undergo abrupt changes in volume in response to external stimuli such as changes in solvent composition¹, pH², electric field³ and temperature^{4–6}. For several of the potential applications of these materials, such as 'smart' actuators, a fast response is needed. The kinetics of swelling and de-swelling in these gels are typically governed by diffusion-limited transport of the polymeric components of the network in water, the rate of which is inversely proportional to the square of the smallest dimension of the gel^{7–9}. Several strategies have been explored for increasing the response dynamics^{10–14}, such as introducing porosity¹⁴. Here we show that we can induce rapid de-swelling of a polymer hydrogel by tailoring the gel architecture at the molecular level. We prepare a crosslinked hydrogel in which the polymer chains bear grafted side chains; the latter create hydrophobic regions, aiding the expulsion of water from the network during collapse. Whereas similar gels lacking the grafted side chains can take more than a month to undergo full de-swelling, our materials collapse in about 20 minutes.

Poly(*N*-isopropylacrylamide) (PIPAAm) is soluble in aqueous media at solution temperatures below 32 °C, its critical solution temperature¹⁵. Above this point, it undergoes a discontinuous phase transition, precipitating from solution suddenly and reversibly over a narrow temperature range^{1,16,17}. In contrast to conventional crosslinked PIPAAm hydrogels, we have prepared a thermosensitive hydrogel with a comb structure in which PIPAAm chains are grafted onto crosslinked networks (Fig. 1). Within the gel, terminally grafted chains have freely mobile ends, distinct from the typical network structure in which both ends of the PIPAAm chains are crosslinked and relatively immobile. With increasing temperature, grafted PIPAAm chains begin to collapse from their expanded (hydrated) form to compact (dehydrated) forms. This collapse occurs before the PIPAAm network begins to shrink, because of the mobility of the grafted chains. The grafted polymer chains dehydrate to create hydrophobic nuclei which enhance aggregation of the crosslinked chains.

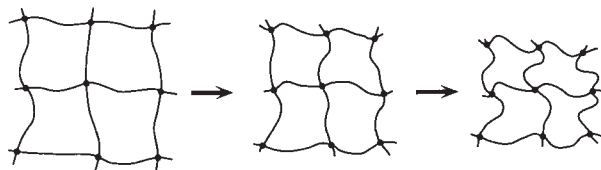
The transmittance of PIPAAm aqueous solution changes rapidly because of conformational changes over a small temperature change^{15,17}. We have previously observed changes from hydro-

Received 3 November 1994; accepted 6 February 1995.

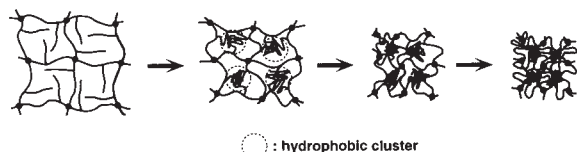
1. Sagan, C. & Dermott, S. F. *Nature* **300**, 731–733 (1982).
2. Fiasar, F. M. *Science* **221**, 55–57 (1983).
3. Lunine, J. I., Stevenson, D. J. & Yung, Y. K. *Science* **222**, 1229–1230 (1983).
4. Lunine, J. I. *Rev. Geophys.* **31**, 133–149 (1993).
5. Muhleman, D. O., Grossman, A. W., Butler, B. J. & Slade, M. A. *Science* **248**, 975–980 (1990).
6. Muhleman, D. O., Grossman, A. W., Slade, M. A. & Butler, B. J. (abstr.) *Bull. Am. astr. Soc.* **24**, 954–955 (1992).
7. Grossman, A. W. & Muhleman, D. O. (abstr.) *Bull. Am. astr. Soc.* **24**, 954 (1992).
8. Lemmon, M. T., Karkoschka, E. & Tomasko, M. *Icarus* **103**, 329–332 (1993).
9. Griffith, C. A. *Nature* **364**, 511–514 (1993).
10. Smith, P. H., Lemmon, M. T., Caldwell, J. J., Allison, M. D. & Sromovsky, L. A. (abstr.) *Bull. Am. astr. Soc.* **26**, 1181 (1994).
11. Sears, W. D. (abstr.) *Bull. Am. astr. Soc.* **26**, 1184 (1994); *Icarus* (in the press).
12. Lambeck, K. *The Earth's Variable Rotation: Geophysical Causes and Consequences* 295 (Cambridge Univ. Press, Cambridge, 1980).
13. Webb, D. J. *Contemp. Phys.* **23**, 419–442 (1982).
14. Burns, J. A. in *Satellites* (eds Burns, J. A. & Matthews, M. S.) 117–158 (Univ. Arizona Press, Tucson, 1986).
15. Dermott, S. F. *Icarus* **37**, 310–321 (1979).

† To whom correspondence should be addressed.

Homopolymer gel



Comb-type graft polymer gel



○ : hydrophobic cluster

philic to hydrophobic behaviour for PIPAAm-terminally grafted surfaces due to rapid changes in polymer conformation (again, this is attributed to the mobility of grafted PIPAAm¹⁸). PIPAAm-grafted surfaces show hydrophilic properties at low temperatures; as the temperature increases, the contact angle of water also increases, indicating increasingly hydrophobic surface properties. The behaviour of these systems is distinct from that of surfaces on which PIPAAm molecules were attached by anchoring at several points along the chain: the decrease in hydrophilicity with increasing temperature is substantially less for the latter than for surfaces with terminally grafted chains.

Above the phase transition temperature, PIPAAm networks undergo both inter- and intramolecular hydrophobic interactions between alkyl side groups, which induce polymer network aggregation. We have reported previously¹⁹ that hydrophobic butyl methacrylate as a comonomer increases the intrinsic aggregation forces of PIPAAm gels. Typically, a dense collapsed polymer layer rapidly forms on the surface of these hydrophobized gels above their phase transition temperature¹⁹.

The hydrated and expanded grafted PIPAAm chains of our new gels are hydrophilic at low temperature. With increasing temperature, the grafted PIPAAm rapidly starts to dehydrate and becomes more hydrophobic. This thermally induced dehydration of the grafted PIPAAm chains promotes rapid shrinking of the crosslinked network.

We prepared comb-type PIPAAm grafted gels as follows: first, we synthesized semitelechelic (that is, having one functional end group per polymer chain) PIPAAm with a terminal amino end group by radical telomerization of the monomer (IPAAm) with 2-aminoethanethiol (AESH) as a chain transfer agent. We dissolved 13.4 g of purified IPAAm, 0.128 g of AESH and 0.0197 g of *N,N'*-azobisisobutyronitrile as an initiator in 50 ml of distilled *N,N*-dimethylformamide (DMF). The ampoule containing the solution was sealed by conventional methods and immersed in a water bath held at 75 °C for 15 h. After concentrating the

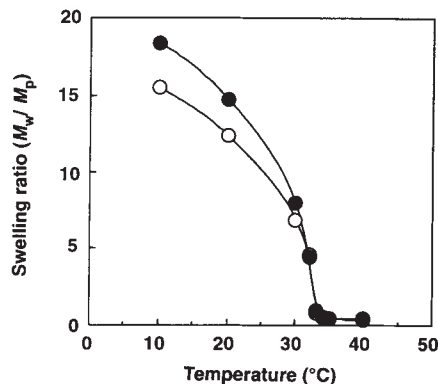
FIG. 1 Structure and shrinking mechanisms for conventional homopolymer and comb-type grafted PIPAAm gels undergoing temperature-induced collapse in aqueous media.

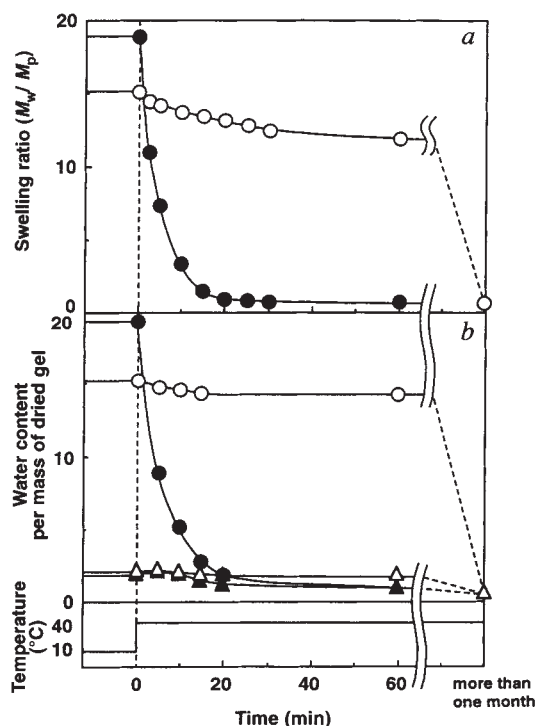
reactant by DMF evaporation, the reactant was poured into diethyl ether to precipitate the synthesized semitelechelic PIPAAm. The PIPAAm product was collected over a filter and purified by repeated precipitation in diethyl ether. The number-average and mass-average relative molecular masses determined by gel permeation chromatography in tetrahydrofuran at 40 °C (against polystyrene standards) were 14,000 and 19,000, respectively. A polymerizable end group was introduced into the semitelechelic amino PIPAAm by reacting 2 g of the amino-semitelechelic PIPAAm with 0.4 g of *N*-acryloxysuccinimide in 30 ml of DMF at 4 °C for 2 days.

To synthesize comb-type PIPAAm gels, we dissolved 1.09 g of IPAAm monomer, 0.468 g of semitelechelic PIPAAm containing a terminal acrylate group, 0.0266 g of *N,N'*-methylenebisacrylamide as a crosslinker and 48 µl of tetramethylethylenediamine as an accelerator in 10 ml of distilled water, and bubbled the solution with dry nitrogen gas for 10 minutes. Ammonium persulphate (8 mg, initiator) was added to the solution, and then the solution was injected between two Mylar sheets separated by a Teflon gasket (2.0 mm thick) and backed by glass plates. The solution was polymerized at 15 °C for 1 day. We immersed the gel membranes formed in pure water to remove unreacted compounds for 5 days, changing the water every day. The swollen gel membrane was cut into disks (15 mm diameter) using a cork borer and dried under ambient conditions for 1 day and under vacuum for 5 days at room temperature. The prepared grafted PIPAAm hydrogel is transparent, suggesting that the network structure is homogeneous on lengthscales above visible wavelengths and that the PIPAAm macromonomer radicals are active enough to copolymerize readily with small IPAAm monomers.

Measurement of equilibrium swelling ratios for the gels in water over a series of temperatures shows that the comb-type PIPAAm graft gel has the same phase transition temperature (32 °C) as the IPAAm homopolymer gel containing the same

FIG. 2 Equilibrium swelling ratio of homopolymer (○) and comb-type grafted PIPAAm (●) gels in water as a function of temperature. The swelling ratio is defined as the mass of absorbed water per mass of dried polymer disk (M_w/M_p).





amount of IPAAm (Fig. 2). Below this transition temperature, the comb-type graft gel shows slightly more swelling than the homopolymer gel. We speculate that the comb-type gel becomes more hydrated because of the inherent mobile nature of grafted PIPAAm chains, which have free ends that are readily exposed to water.

Disks of comb-type graft PIPAAm gels and IPAAm homopolymer gels with identical thicknesses and diameters show different de-swelling kinetics when the temperature is increased from below to above the phase transition temperature (Fig. 3a). Conventional IPAAm homopolymer gels shrink very slowly after the temperature is increased from 10 °C to 40 °C, requiring more than a month to reach equilibrium. This gel shrinks gradually from the surface inwards, mediated by diffusion of the collapsing polymer network and the release of entrapped water from the collapsing gel. As a dense, collapsed polymer layer impermeable to water is formed near the gel surface before bulk gel collapse is initiated (thermal convection is more rapid than mass transfer), gel shrinking is hindered after the initial stages by internal hydrostatic pressure^{20,21}. As a result, the PIPAAm homopolymer gel shrinkage rate is limited by water permeation from the gel interior through the collapsed polymer skin, keeping water within the gel for longer periods.

In contrast to the IPAAm homopolymer gel, the comb-type PIPAAm graft gel shrinks rapidly to its equilibrium state. In the process, the gel undergoes large, rapid volume changes with marked mechanical buckling, indicative of the much greater aggregation forces operating within the grafted gel. Trapped water is rapidly squeezed out from the gel interior. This is sup-

FIG. 3 a, Shrinking kinetics for homopolymer (○) and comb-type grafted PIPAAm (●) gels. The disk-shaped IPAAm homopolymer gel and the comb-type graft polymer gel (diameter 15 mm, thickness 2 mm) were first equilibrated in pure water at 10 °C. Gels were then quickly moved into water at 40 °C (the heating history is shown at the bottom of the figure). At specific times these gels were removed from the water and weighed after being wiped with filter paper to remove excess water on the surface. The shrinking kinetics are defined as the changes with time in the swelling ratios for the gels. b, Changes in water structure for shrinking homopolymer (○, freezable water; △, non-freezable water) and comb-type grafted PIPAAm (●, freezable water; ▲, non-freezable water) gels at 40 °C. Two types of gel disks equilibrated at 10 °C (diameter 15 mm, thickness 2 mm) in pure water were quickly transferred into water at 40 °C. The gels were cut into disks (4 mm diameter at centre) at predetermined times using a cork borer. After wiping excess water from the surface, the samples were sealed in aluminium pans and placed in a differential scanning calorimeter (Mettler TA-3000 system). After cooling to -20 °C within 5 min, the samples were heated to 40 °C at the rate of 1 °C min⁻¹. The endothermal heat of water in the gels was measured using an empty aluminium pan as a reference. From the integral of the endothermal peak for water melting (near 0 °C), the gel freezable water content was determined. Total water content was determined from the mass difference between the swollen gel and the dried gel. Non-freezable water content, restricted in its molecular mobility by interaction with hydrated polymer chains, was calculated from the difference between total and freezable water content for these gels.

ported by the changes in the amount of freezable water within two types of gel matrices determined by DSC. As can be seen in Fig. 3b, about 90% of the freezable water was desorbed from the graft-type PIPAAm gel within 20 min after the temperature was increased to 40 °C, although non-freezable water content remains nearly constant and fairly low. Therefore, we attribute the marked swelling changes observed for graft-type PIPAAm gel to the large change in freezable water content in the gel. In contrast to the graft-type PIPAAm gel, only 5% of the freezable water was desorbed from the IPAAm homopolymer gel after 60 min. Rapid shrinking of the graft-type PIPAAm gel is due to the immediate dehydration of PIPAAm grafted chains in the gel matrix followed by subsequent hydrophobic interactions between dehydrated grafted chains preceding shrinkage of the PIPAAm network, affecting rapid expulsion of water from the gel matrix. The rapid shrinking and release of most of the freezable water results in a large volume change, which suggests that a skin structure that would reduce the de-swelling rate is not formed in this case. An increase in void volume within the grafted PIPAAm network resulting from collapsed grafted chains may also contribute to rapid release of water to the gel exterior.

In the case of a gel swelling in water at 10 °C from an equilibrium shrunken state (40 °C), the swelling rate was slower than the de-swelling rate, and no difference in swelling rate was observed between the two types of gel. In both cases the amount of absorbed water increases in proportion to the square root of time. These results indicate that polymer network diffusion is rate-determining for swelling. The details of this process are currently under investigation. □

Received 30 June 1994; accepted 6 February 1995.

- Hirokawa, E. & Tanaka, T. *J. chem. Phys.* **81**, 6379–6380 (1984).
- Tanaka, T. *et al. Phys. Rev. Lett.* **45**, 1636–1639 (1980).
- Tanaka, T., Nishio, I., Sun, S.-T. & Ueno-Nishio, S. *Science* **218**, 467–469 (1981).
- Okano, T., Yui, N., Yokoyama, M. & Yoshida, R. in *Japanese Technology Reviews Section E* Vol. 4 (eds Ikoma, T. *et al.*) 67–105 (Gordon Science, Yverdon, Switzerland, 1993).
- Hoffman, A. S. *J. Controlled Release* **6**, 297–305 (1987).
- Dusek, K. (ed.) *Responsive Gels: Volume Transitions II* (Springer, Berlin, 1993).
- Tanaka, T. & Fillmore, D. J. *J. chem. Phys.* **70**, 1214–1218 (1979).
- Tanaka, T., Sato, E., Hirokawa, Y., Hirotsu, S. & Peetermans, J. *Phys. Rev. Lett.* **55**, 2455–2458 (1985).
- Sato Matsuo, E. & Tanaka, T. *J. chem. Phys.* **89**, 1695–1703 (1988).
- Hirasa, O., Ito, S., Yamauchi, A., Fujishige, S. & Ichijo, H. in *Polymer Gels* (eds DeRossi, D. *et al.*) 247–256 (Plenum, New York, 1991).

- Suzuki, M. in *Polymer Gels* (eds De Rossi, D. *et al.*) 221–236 (Plenum, New York, 1991).
- Kabra, B. G. & Gehrke, S. H. *Polym. Commun.* **32**, 322–323 (1991).
- Wu, X. S., Hoffman, A. S. & Yager, P. J. *Polym. Sci., A. Polym. Chem.* **30**, 2121–2129 (1992).
- Dong, L. C. & Hoffman, A. S. *J. Controlled Release* **13**, 21–31 (1990).
- Heskins, M., Guillet, J. E. & James, E. J. *Macromol. Sci. Chem.* **A2**, 1441–1455 (1968).
- Bae, Y. H., Okano, T. & Kim, S. W. *J. Polym. Sci. Polym. Phys.* **28**, 923–936 (1990).
- Takei, Y. G. *et al. Bioconj. Chem.* **4**, 341–346 (1993).
- Takei, Y. G. *et al. Macromolecules* **27**, 6163–6166 (1994).
- Yoshida, R., Sakai, K., Okano, T. & Sakurai, Y. *J. Biomater. Sci. Polym. Edn* **6**, 585–598 (1994).
- Yoshida, R. *et al. J. Biomater. Sci. Polym. Edn* **3**, 155–162 (1991).
- Yoshida, R., Sakai, K., Okano, T. & Sakurai, Y. *J. Biomater. Sci. Polym. Edn* **3**, 243–252 (1992).

ACKNOWLEDGEMENTS. We thank D. W. Grainger for comments and discussions.